Corrosion Performance of Embedded Steel in Fly Ash Geopolymer Concrete by Impressed Voltage Method

M.Olivia & H.R. Nikraz
Curtin University, Perth, Western Australia, Australia

ABSTRACT: The present paper covers a study of the corrosion performance of embedded steel in fly ash geopolymer concrete by an accelerated corrosion test set up. Concrete specimens were exposed to a constant impressed voltage of 5V and 30V. Two optimized fly ash geopolymer concrete mixtures were compared with a control mix (OPC concrete) at an equivalent strength grade. Alkalinity reduction by phenolphthalein spray, chloride penetration by $AgNO_3$ spray and half cell potential measurement were also investigated. The accelerated corrosion test was carried out for 28 days. Results indicate that the geopolymer concrete displayed a smaller recorded current and higher electrical resistance than the corresponding control mix. Small cracks were observed in the fly ash geopolymer samples. It can be concluded that the fly ash geopolymer concrete had good corrosion performance and yielded longer time to failure than the OPC concrete.

1 INTRODUCTION

1.1 *Fly ash geopolymer concrete*

Fly ash geopolymer concrete has emerged as a new construction material with some properties equal or better than the OPC concrete. Geopolymer binder has a potential to reduce cement consumption and maximize utilization of waste such as fly ash in concrete production. It was estimated that approximately 14.6 million tons (Mt) of fly ash have been produced in Australia in 2008. Approximately 31.5% (4.5 Mt) of that total has been used in various practical means (ADAA, 2008). Instead of having a positive contribution to waste reduction, the total carbon emission from fly ash geopolymer production was estimated to be approximately 78 kg/m^3. While the total carbon emission for OPC concrete incorporating slag production was 248 kg/m^3 (Wimpenny, 2009). Thus, the fly ash geopolymer concrete can be considered a suitable candidate for sustainable construction material and a low carbon concrete.

Fly ash geopolymer concrete has different final product and microstructure than the OPC concrete. The final product called aluminosilicates, was produced by a chemical reaction between silica and alumina of fly ash with alkaline solutions (Palomo, et al. 1999). Fly ash geopolymer concrete could have high strength properties (Hardjito, 2004) and was reported to be durable in artificial acid (Song, 2005) and sulfate environment (Wallah, 2003).

1.2 *Corrosion study of geopolymer*

Corrosion of steel reinforcement bar embedded in geopolymer material has been an object of study to confirm its technical viability. The available alkalinity of geopolymer material initially was suspected to be harmful for alkali-silica reaction, but then it was found to be beneficial to maintain passivity of the steel bar in concrete (Davidovits, 2005). Morris and Hodges (2005) study of various metals embedded in fly ash geopolymer mortar demonstrated that passive film around the steel bar could be maintained as long as the matrix is alkaline. However, there was no information regarding the available time to maintain the passive film by the matrix. Another research using metakaolin geopolymer as a steel bar coating has shown little corrosion activity by 25% than the steel bar without geopolymer coating (Kriven et al. 2007). The application of geopolymer coating probably affected the interface of steel bar and mortar, and thus the corrosion current.

Yodmunee and Yodsujai (2006) used an impressed voltage test to accelerate the corrosion of fly ash geopolymer concrete by up to 72 hours charging. Geopolymer concrete has shown little corrosion activity than that of the OPC concrete. Another investigation showed that the fly ash geopolymer concrete could passivate steel bars as effectively as the OPC concrete in chloride free environment (Miranda et al.

2005). The matrix still has high pH after reaction which could be one of the reasons for the passivation effect on the steel bar. Recently, Bastidas et al. (2008) found that the chloride also depassivated the steel bar of fly ash geopolymer as fast as the OPC samples. This depends on the type and dosage of activators used, since the composition of fly ash geopolymer matrix could influence the resulting pH.

Current experiments were designed to investigate the reinforced steel bar corrosion of fly ash geopolymer and OPC samples using accelerated corrosion test by charging the steel bar in concrete with two different impressed voltages, i.e. 5V and 30V. Sodium chloride in concentration of 3.5% was used as an electrolyte. Corrosion current, average daily resistance, visual inspection and half cell potential measurement were investigated.

2 EXPERIMENTAL PROGRAM

2.1 *Materials and mix design*

Low calcium fly ash (class F) according to ASTM C618 from Collie power station, Western Australia was used as a primary material of the geopolymer concrete. General purpose Ordinary Portland Cement (OPC) that meets the requirement of AS 2350 was used for the control mix. The chemical composition of fly ash and cement is presented in Table 1.

Coarse and fine aggregates in saturated surface dry conditions were used. A combination of sodium hydroxide and sodium silicate was mixed as alkaline activators in the current research. The sodium hydroxide solution was prepared by diluting NaOH solid with distilled water to obtain 14M solution. The sodium silicate Grade D was supplied by PQ Australia with a specific gravity of 1.52, a modulus silicate ratio (*Ms*) of 2, (where *Ms* = SiO_2/Na_2O, Na_2O = 14.7%, SiO_2 = 29.4%). As an admixture, napthlene sulphonated polymer based superplasticizer from BASF that available commercially was included to improve the workability. Tap water was added as extra water in the mixtures.

The fly ash geopolymer concrete mixtures were designed through optimization by the Taguchi method. The methodology was based on a combination of different factors and levels to produce concrete mixtures with desirable properties in a seawater environment. The full methodology and optimization process is explained in detail elsewhere (Olivia & Nikraz, 2009). The mixture proportions, slump and some concrete properties are presented in Table 2.

2.2 *Mixing and curing*

Geopolymer was made by mixing the dry materials with alkaline activators solution in a 70L pan mixer. All concrete mixtures were cured at a different curing method and temperature. The OPC concrete specimens were demoulded after 24 hours. They were

Table 1. Chemical composition of fly ash and cement.

Oxides	Fly ash	Cement
	wt (%)	wt (%)
Silica (SiO_2)	50.50	21.10
Alumina (Al_2O_3)	26.57	4.70
Calcium Oxide (CaO)	2.13	63.80
Ferric oxide (Fe_2O3)	13.77	2.80
Potassium oxide (K_2O)	0.77	-
Magnesium oxide (MgO)	1.54	2.00
Sodium oxide (Na_2O)	0.45	0.50
Phosporus pentoxide (P_2O_5)	1.00	-
Sulphuric anhydride (SO_3)	0.41	2.50
Loss on ignition (LOI)	0.60	2.10
Chloride	-	0.01

Table 2. Mixture proportions and some properties of concrete.

Mix type	T7	T10	OPC
Fly ash (kg/m^3)	424.6	498.5	-
Cement (kg/m^3)	-	-	422.5
Aggregates (kg/m^3)	1848.0	1752.0	1788.3
NaOH 14M (kg/m^3)	36.4	42.7	-
Sodium silicate (kg/m^3)	91	107	-
Superplasticizer (kg/m^3)	6.4	7.5	-
Water (kg/m^3)	17.9	18.8	190
Slump (mm)	180	-	90
Compressive strength (MPa)			
28 days	56.29	60.03	56.22
91 days	53.97	63.29	65.15
Tensile strength (MPa)			
28 days	4.13	3.37	3.97
91 days	4.18	4.29	4.25
Water absorption (%)			
28 days	3.79	4.33	5.09
91 days	3.45	3.73	5.14
Sorptivity (mm/min$^{0.5}$)			
28 days	0.1026	0.1354	0.1888
91 days	0.1624	0.1264	0.2027
pH			
28 days	11.38	11.37	12.40
91 days	11.32	11.36	n/a

placed in the water immediately after demoulding. The moist curing was carried out for 28 days. The specimens were taken out from the ponds and left air dried in the curing room until testing date. The geopolymer concrete specimens were steam cured for two different curing regimes. Mix T7 was cured in the steam curing chamber for 12 hours at 70°C, while mixes T10 was steam cured at 75°C for 24 hours. The specimens were left air cured in the curing room with temperature of 23-25°C.

2.3 *Impressed voltage method*

An impressed voltage system was used to accelerate corrosion process. Corrosion test samples were 100x200mm cylinders with 16mm diameter steel bars located in the middle of specimen (lollipop). The setting up adopted a potentiostatic method to study initiation, propagation and repassivation of localized corrosion (ASM, 1989). The same procedure was used by various researchers (Guneyisi, et al. 2005; Sakr, 2005). In the present research, a constant voltage of 5V and 30V was induced to the system.

The system consisted of a power supply, resistor and data logger. A stainless steel plate was located around the specimens. The bar was connected to the positive terminal in the power supply, while the steel plate was connected to the negative terminal. The steel reinforcing bar acted as an anode, whereas the stainless plate was a cathode. The specimens were immersed in 3.5% sodium chloride solution for 3 days before the test date. After pre-immersion, those specimens were placed in a container contained electrolyte solution. The set up is illustrated in Figure 1.

Based on the recorded current, the theoretical average daily resistance can be determined by Ohm's Law:

$$R_{avg} = \frac{V_{constant}}{I_{avg}} \quad (1)$$

where $V_{constant}$ = the voltage; and I_{avg} = the recorded current.

2.4 *Chloride penetration and residual alkalinity*

Chloride penetration into the concrete was measured by spraying $AgNO_3$ solution (Otsuki et al. 1999). Samples were split off and 0.1N $AgNO_3$ solution was sprayed to the surface of the concrete. The depth of chloride penetration could be noticed from color change by white precipitate in the region of silver chloride formation. The free chloride area shows brown color.

Residual alkalinity was assessed by spraying phenolphthalein solution (1% phenolphthalein in 70% ethyl alcohol) to the split surfaces. Phenolphthalein is used to measure pH of carbonated concrete (RILEM, 1988). Non-carbonated concrete turns red, while the carbonated concrete is colorless. The same method was used to check concrete pH by splitting the core of concrete and spray it with the phenol solution (Mattila & Pentti, 1996). The resulted red or pink color has pH in the range of 8.2-9.8.

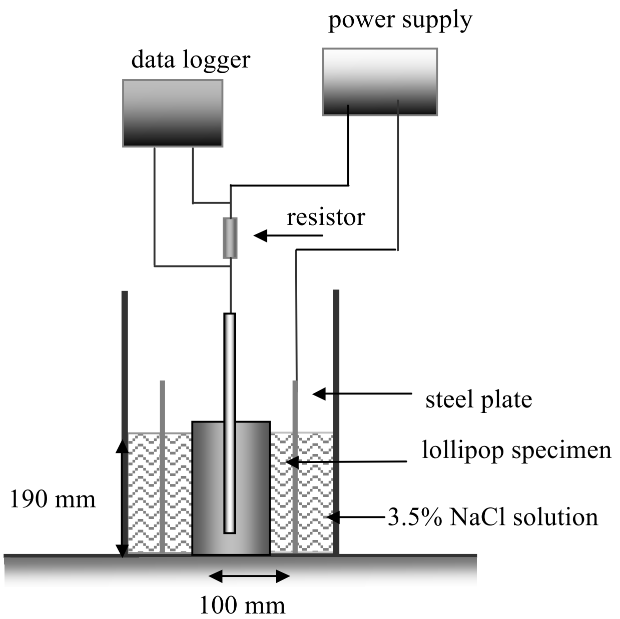

Figure 1. Accelerated corrosion set up.

2.5 *Half cell potential measurement*

A probability of steel corrosion at various ages was carried by half cell potential measurement. The steel bar and a reference electrode (Ag/AgCl) were connected to an auto range high impedance digital multi meter. The half cell potential measurement followed ASTM C-876. The lollipop cylinders were immersed in 3.5% sodium chloride and the potentials reading were taken at 1, 3, 7, 14, 21, 28, 56, and 91 days.

3 RESULTS AND DISCUSSIONS

3.1 *Corrosion current*

Figure 2 shows the recorded current with time for the geopolymer and OPC concrete at the constant voltage of 5V. It can be seen that the corrosion activity of the OPC concrete was higher than the geopolymer concrete. The trend of current versus time plot at the constant voltage of 30V indicates high current readings for the OPC concrete shortly before samples crack (Fig. 3). Current initially decreased for the first few days for the geopolymer concrete samples, and then was followed by a gradual increase of current with several oscillations. According to Yodmunee and Yodsujai (2006) and Kriven (2007), the recorded current of the geopolymer concrete was smaller than the OPC concrete, that closely aligns with the current findings. In general, the impressed voltage value in the system is found useful to induce corrosion activity at a different rate for both type of concrete.

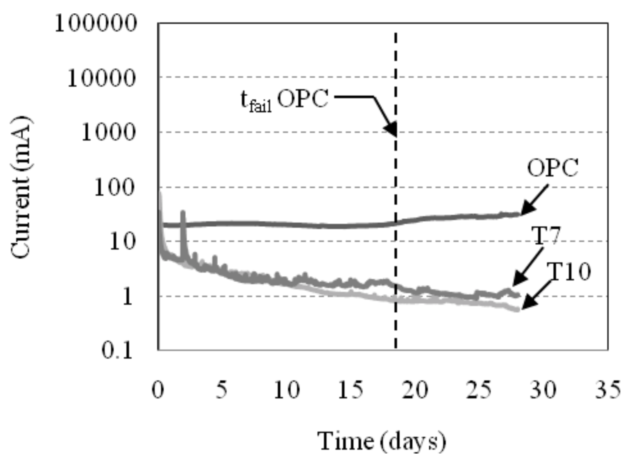

Figure 2. Corrosion current-time relationship at constant voltage of 5V.

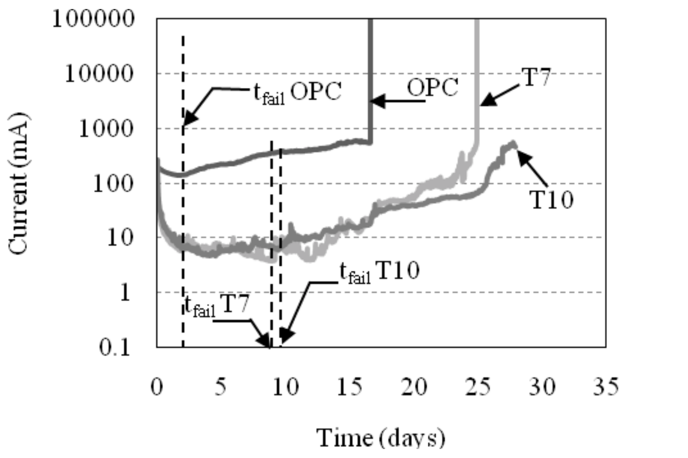

Figure 3. Corrosion-current time relationship at constant voltage of 30V.

The time to failure (t_{fail}) for specimens is defined as time corresponding to the onset of a large increase in current (Florida Method, 2000). It can be observed from Figure 3, that the OPC specimens had the shortest time to failure, followed by the geopolymer mix T7 and T10 at 8.7 and 9.2 days, respectively. Time to failure was not apparent for both geopolymer samples with a constant voltage of 5V. t_{fail} was longer for the OPC concrete at an impressed voltage of 5V (Fig. 2). The summary of corrosion current and time to failure values is presented in Table 3. Both type of concrete has notable differences on the initial and final current level.

The magnitude of current and the time to failure of the OPC concrete depends on the type of mix and solution. The specimens reach active corrosion potentials and crack under impressed voltage. The presence of chloride ions was obvious to depassivate the protecttive film of the embedded steel bar. On the other hand, it is interesting to note the geopolymer matrix could delay the effect of impressed voltage to accelerate the corrosion process. The available alkalinity in the pore solution of fly ash geopolymer concrete might reduce the effect of the depassivation by the chloride ions. It was found that there was sufficient alkalinity to passivate the embedded steel observed in the fly ash geopolymer pore solution (Llyod et al. 2010). However, it is important to have sufficient low permeability to prevent alkali leaching out from the matrix with time, since the fly ash geopolymer system could not refill the pore solution once the alkali is removed.

3.2 *Theoretical average daily resistance (Ohm's Law)*

The average daily resistances of OPC and geopolymer samples were calculated from Ohm's Law (Equation 1) are presented in Figure 4 and 5. The value of average daily resistance at the time to failure could be seen in Table 4. Both graphs demonstrate that the electrical resistance of fly ash geopolymer

Table 3. Current reading and time to failure of samples at constant voltage of 5V and 30V.

Mix	Initial current (mA)		Final current (mA)		Time to failure (days)	
	5V	30V	5V	30V	5V	30V
T7	31.38	218.04	1.04	99999.99	n/a	8.77
T10	76.54	268.02	0.17	66.33	n/a	9.22
OPC	23.79	163.64	32.43	99999.99	14.7	2.27

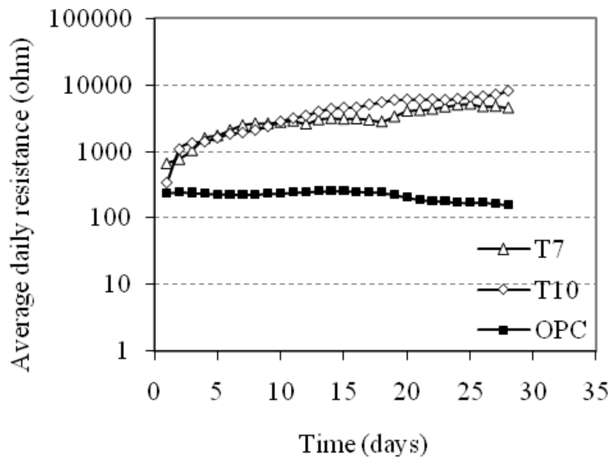

Figure 4. Variation of concrete average daily resistance with time at constant voltage of 5V.

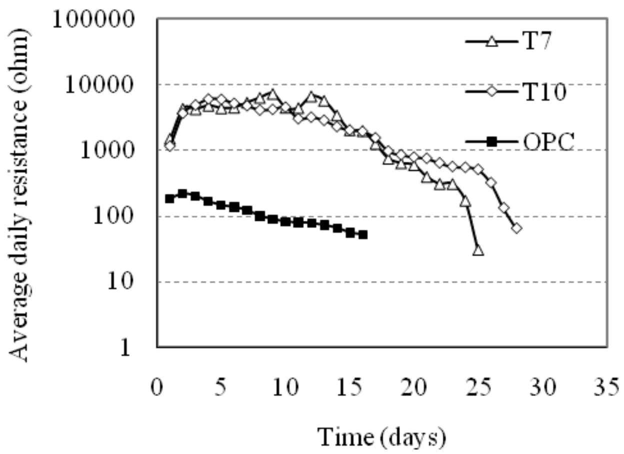

Figure 4. Variation of concrete average daily resistance with time at constant voltage of 30V.

Table 4. Time to failure and resistance of samples at voltage of 30V.

Mix	Time to failure (days)	Resistance (k-ohm)
T7	8.77	4.25
T10	9.22	6.22
OPC	2.27	0.14

concrete was higher than that of the OPC concrete in when the time to failure was achieved.

Electrical properties of concrete or resistance are influenced by the mixture composition and hydration process of cement-based materials. Geopolymer primary source is fly ash, which has an effect on the

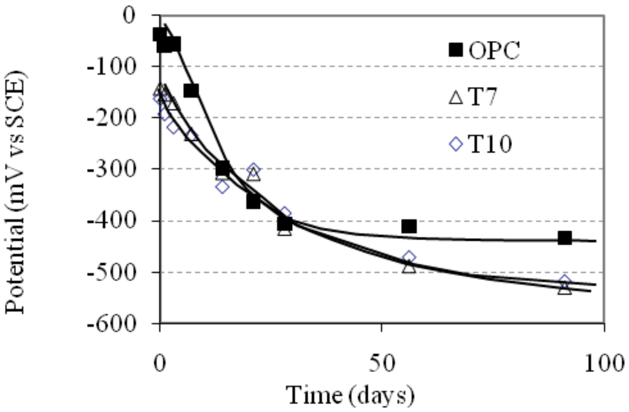

Figure 5. Half cell potential reading for the OPC and geopolymer concrete up to 91 days.

electrical resistance of concrete (Cabrera, 1996). Inclusion of fly ash can increase the geopolymerization process and resistivity of geopolymer cement pastes (Zhang et al. 2009). The current results clearly illustrate the high electrical resistance of the fly ash geopolymer concrete matrix, demonstrated previously by Morris & Hodges (2005). A positive impact from the high electrical resistance of concrete surrounding the steel bar between anode and cathode is a reduction of the rate of charge-carrying ionic species flow (Bentur, 1997).

3.3 *Half cell potential reading*

The half cell potential reading was taken as an average value of three specimens (Fig. 6). The corrosion potential was high at the initial stage of concrete exposure. The geopolymer concrete showed more negative (lower) potentials than the OPC concrete. Both the geopolymer and OPC concrete showed potential readings more negative than -270mV. According to the ASTM Standard (2009), the half cell potential value less than -270mV shows 90% probability of corrosion risk. The possibility of passive films being developed or destroyed cannot be assumed because the data taken is only up to 91 days of measurement.

3.4 *Visual inspection*

The samples were split off at the end of the test session. The condition of concrete surface and interface of steel-concrete were observed. The OPC concrete sample showed a typical wide crack, a high degradation of matrix and high mass loss of steel bar. When the phenolphthalein indicator was sprayed, there was a strong pink color on the concrete surface or no sign of alkalinity reduction during the test. Chloride has penetrated highly into the steel bar as indicated by spraying the $AgNO_3$ solution.

Figure 7 illustrates the area near the top rebar and its trace after dissection revealed one or more local sites where corrosion product (rust) was available.

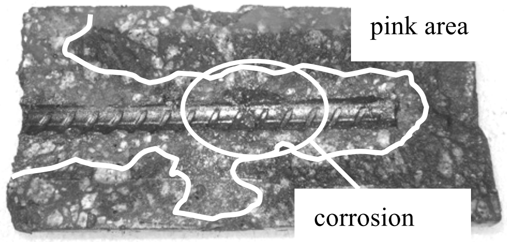

Figure 7. Alkalinity residual of concrete around the steel bar (T7 specimen) after exposed to constant voltage of 30V.

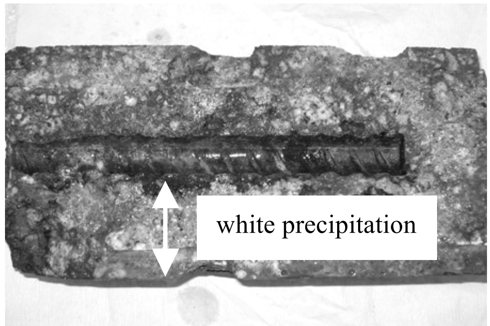

Figure 8. Chloride ion penetration into concrete (T7 specimen) after exposed to constant voltage of 30V.

There was no sign of bonding between steel and concrete. Black thick product covered the steel bar, which soon turned to brown rust when in contact with air. There was alkalinity reduction around the steel bar as indicated by light color area inside the white line (Fig. 7). Chloride was thoroughly penetrated into the steel bar as indicated by $AgNO_3$ solution. Light grey area showed a distribution of silver chloride precipitation on the concrete (Fig. 8).

Small cracks were observed on the surface of fly ash geopolymer concrete. Some corrosion products filled the nearest voids in the embedded steel and concrete interface section. Gradually, the rust filled the concrete pores around the steel bar. The available voids and interconnected pores are able to reduce the pressure required to produce crack propagation of the geopolymer concrete. This might be a reason of only small cracks were spotted on the surface of fly ash geopolymer concrete specimens. This condition is not favorable in application because the corrosion activity can be extended in order to generate significant pressure, thus, will result in high overall loss of steel bar (Allan, 1995). However, since the actual mass losses of steel bar and corrosion rates of fly ash geopolymer concrete are not presented in the current research, it is still considered early to justify the assumption.

4 CONCLUSIONS

The corrosion performance of embedded steel bar in fly ash geopolymer was studied by impressed voltage method. It was found the magnitude of the voltage is only effective to induce corrosion activity at a different rate. The geopolymer concrete shows a low recorded current level and higher electrical resistance than the corresponding control mix. The existing alkalinity on the matrix pore solution could be a reason of this behaviour. Small cracks were spotted on the surface of fly ash geopolymer concrete specimens without significant increase on the recorded current. Visual inspection on the geopolymer dissected samples shows that there was an alkalinity reduction around the steel bar, high chloride ion penetration into the geopolymer concrete and no severe damage on the steel bar. It can be concluded that the fly ash geopolymer concrete had good corrosion performance and yielded longer time to failure than the OPC concrete by using impressed voltage method.

5 REFERENCES

ADAA, 2008. *ADAA Statistics Page*. http://www.adaa.asn.au/statistics.htm (accessed May 20, 2010).

Allan, M.L. 1995. Probability of corrosion induced cracking in reinforced concrete. *Cement and Concrete Research* 25(6): 1179-1190.

American Society for Metals. 1989. *Metals Handbooks*. Ohio: American Society for Metals.

ASTM Standard. 2009. Standard Test Method for Half-Cell Potentials of Uncoated Reinforcing Steel in Concrete. ASTM C876-09. http://www.astm.org (accessed December 10, 2009).

Bastidas, D.M., Fernandez-Jimenez, A., Palomo, A. & Gonzalez, J.A. 2008. A study on the passive state stability of steel embedded in activated fly ash mortars. *Corrosion Science* 50(4): 1058-1065.

Bentur, A., Diamond, S. & Berke, N.S. 1997. *Steel corrosion in concrete*. London: E & FN Spon.

Cabrera, J.G.1996. Deterioration of concrete due to reinforcement steel corrosion. *Cement and Concrete Composites* 18 (1): 47-59.

Davidovits, J. 2005. Geopolymer chemistry and sustainable development. The poly(sialate) terminology: a very useful and simple model for the promotion and understanding of green-chemistry. In Joseph Davidovits (ed.), *World Congress Geopolymer 2005: Geopolymer, Green Chemistry and Sustainable Development Solutions; Proc. intern. conf., Saint-Quentin, 28 June -1 July 2005.* Saint-Quentin: Institute Geopolymere.

Florida Method. 2000. Florida method of test for an accelerated laboratory method for corrosion testing of reinforced concrete using impressed current. FM 5-522. http://www.dot.state.fl.us/statematerialsoffice/administration/library/publications/fstm/methods/fm5-522.pdf (accessed August 30, 2009).

Guneyisi, E., Ozturan, T. & Gesoglu, M., 2005. A study on reinforcement corrosion and related properties of plain and blended cement concretes under different curing conditions. *Cement and Concrete Composites* 27(4): 449-461.

Hardjito, D., Wallah, S.E., Sumajouw, D.M.J, & Rangan, B.V. 2004. On the development of fly ash based geopolymer concrete. *ACI Materials Journal* 101(6): 467-472.

Kriven, W.M., Gordon, M., Ervin, B.L. & Reis, H. 2008. Corrosion protection assessment of concrete reinforcing bars with a geopolymer coating. In Manuel Brito, Eldon Case, Waltraud M. Kriven (eds.), *Developments in Porous, Biological and Geopolymer Ceramics, Ceramic Engineering and Science Proceedings* 28(9): 373-382; *Proc. intern. conf., Daytona Beach, 21-26 January 2007.* New Jersey: John Wiley & Sons.

Llyod, R.R., Provis, J.L. & van Deventer, J.S.J. Pore solution composition and alkali diffusion in inorganic polymer cement. *Cement and Concrete Research* 40(9): 1386-1392.

Mattila, J. S. & Pentti, M.J. 1996. Re-alkalisation of carbonated concrete by cement-based coatings. In Page, C., Bamforth, P., & Figg, J. (eds.), *Fourth International Symposium on Corrosion of Reinforcement in Concrete Construction; Proc. Intern. symp., Cambridge, 1-4 July 1996*. Cambridge: The Royal Society of Chemistry.

Miranda, J.M., Fernandez-Jimenez, A., Gonzalez, J.A. & Palomo, A. 2005. Corrosion resistance in activated fly ash mortars. *Cement and Concrete Research* 35(6): 1210-1217.

Morris, J., & Hodges, S. 2005. Corrosion of metals in fly ash-based geopolymers. In Joseph Davidovits (ed.), *World Congress Geopolymer 2005: Geopolymer, Green Chemistry and Sustainable Development Solutions; Proc. intern. conf., Saint-Quentin, 28 June -1 July 2005.* Saint-Quentin: Institute Geopolymere.

Olivia, M. & Nikraz, H. 2009. Optimization of fly ash geopolymer concrete mixtures in seawater environment. In Ian Gilbert (ed.), *Proc. of Concrete Solutions 09; Proc. intern. conf., Sydney, 17-19 September 2009*. Sydney: Concrete Institute of Australia.

Otsuki, N., Nagataki, S. & Nakashita, K. 1992. Evaluation of AgNO3 solution spray method for measurement of chloride penetration into hardened cementitious matrix materials. *ACI Materials Journal* 89(6): 587-592.

Palomo, A. Grutzeck, M.W. & Blanco, M.T. 1999. Alkali-activated fly ashes. A cement for the future. *Cement & Concrete Research* 29(8): 1323-1329.

RILEM. 1988. CPC-18 Measurement of hardened concrete carbonation depth. *Materials and Structures* 21**:** 453-455.

Sakr, K. 2005. Effect of cement type on the corrosion of reinforcing steel bars exposed to acidic media using electrochemical techniques. *Cement and Concrete Research* 35(9): 1820-1826.

Song, X., Marosszeky, M., Brungs, M. & Munn, R. 2005. Durability of fly ash based geopolymer concrete against sulphuric acid attack. *In the Proc. of 10DBMC International Conference on Durability of Building Materials and Components, Lyon, 17-20 April 2005.*

Wallah, S.E., Hardjito, D., Sumajouw, D.M.J. & Rangan, B.V. 2003. Sulfate resistance of fly ash based geopolymer concrete. *Proc. of Concrete in the 3rd Millenium; Proc. intern. conf., Brisbane, 17-19 July 2003.* Brisbane: Concrete Institute of Australia.

Wimpenny, D. 2009. Low carbon concrete- options for the next generation of infrastructure. In Ian Gilbert (ed.), *Proc. of Concrete Solutions 09; Proc. intern. conf., Sydney, 17-19 September 2009*. Sydney: Concrete Institute of Australia.

Yodmunee, S. & Yodsujai, W. 2006. Study on corrosion of steel bar in fly ash based geopolymer concrete. *In the Proc. of International Conference on Pozzolan, Concrete and Geopolymer; Proc. intern. conf., Khon Kaen, May 24-25 2006.* Khon Kaen: Sustainable Infrastructure Research and Development Center.

Zhang, Y., Li, Z., Sun, W. & Li, W. Setting and hardening of geopolymeric cement pastes incorporated with fly ash. *ACI Materials Journal* 106(5): 405-412.